

# SUPERTOROID-BASED CHARACTERIZATION OF CARDIAC DIFFUSION TENSOR FIELDS

C. Mekkaoui<sup>1</sup>, M. P. Jackowski<sup>2</sup>, and A. J. Sinusas<sup>1</sup>

<sup>1</sup>Yale University, New haven, CT, United States, <sup>2</sup>University of Sao Paulo, Brazil

## Introduction

Characterization of biological tissue structure and organization using Diffusion Tensor (DT) Magnetic Resonance Imaging (MRI) relies on effective analysis and multidimensional data visualization methods. The toroid-based representation of the DT has been experimentally demonstrated to be less prone to visual ambiguity [1] and offers additional quantitative scalar maps to evaluate the diffusivity and the degree of anisotropy [2]. The purpose of this work is to introduce the *supertoroids*, which are the natural evolution of the toroid-based model to address the limitations of the superquadrics [3] and toroidal glyphs, by unifying the specific advantages of each representation. The methodology is applied on DT-MRI datasets of a normal and infarcted canine hearts. Results indicate that supertoroids enhance cardiac myofiber structure characterization compared to ellipsoidal, superquadrics and toroids.

## Methodology

The supertoroid is a geometric primitive that incorporates the visual features conveyed by the increase in genus inherent to the toroids and a continuum that fully encodes the local eigensystem intrinsic to the superquadrics. **Supertoroidal representation:** The supertoroidal parametric equation is a function of the geometric shape metrics  $C_L = (\lambda_1 - \lambda_2)/\lambda_1 + \lambda_2 + \lambda_3$ ,  $C_P = 2(\lambda_2 - \lambda_3)/\lambda_1 + \lambda_2 + \lambda_3$ , and  $C_S = 3\lambda_3/\lambda_1 + \lambda_2 + \lambda_3$  [4] and is parameterized as follows:

$$C_S \geq C_P \Rightarrow \mathfrak{S}(\theta, \phi) = (\cos^{\eta_1} \theta \{ (C_L + C_P) + C_S \cos^{\eta_2} \phi \} \sin^{\eta_1} \theta \{ (C_L + C_P) + C_S \cos^{\eta_2} \phi \} \sin^{\eta_2} \phi).$$

$$C_S < C_P \Rightarrow \mathfrak{S}(\theta, \phi) = (\cos^{\eta_1} \theta \{ C_S + (C_L + C_P) \cos^{\eta_2} \phi \} \sin^{\eta_1} \theta \{ C_S + (C_L + C_P) \cos^{\eta_2} \phi \} \sin^{\eta_2} \phi).$$

where  $\mathfrak{S}$ , the parameterized glyph surface, is a function of both azimuthal  $\theta \in [0, 2\pi]$  and polar  $\phi \in [0, 2\pi]$  coordinates. The parameters  $\eta_1 = (1 - C_P)^{\eta_1}$  and  $\eta_2 = (1 - C_S)^{\eta_2}$  produce a smooth transition between supertoroidal glyphs, where  $\gamma_1$  controls the shape of the toroidal ring and  $\gamma_2$  the cross-section of the glyph. The role of  $\gamma_1$  and  $\gamma_2$  is to highlight differences in the eigenvalues by varying the sharpness of the edges and the shape cross-section, respectively.

**Data acquisition:** After the animals were euthanized, hearts were excised and perfused with saline. Each heart was then placed and positioned in a container and filled with Fomblin (Ausimont, Thorofare, NJ). DT-MRI data were collected with a 3.0T scanner (Siemens, Erlangen, Germany) using a segmented EPI sequence. An icosahedral diffusion encoding gradient scheme containing 6 directions was applied with a constant b-value=600s/mm<sup>2</sup>. A single image with a b-value=0s/mm<sup>2</sup> was also obtained. Fifty short-axis image slices with resolution 2x2x2mm<sup>3</sup> were acquired with TR=5400ms and TE=84ms. In order to increase SNR, a total of 32 averages were performed over 6 hours and the EPI factor was set to 7.

## Results

Supertoroidal fields were computed in a cross-section of a normal canine heart from a diffusion dataset and compared to the other representations (**Fig.1**). **Fig.1A** shows a short-axis T2-weighted image and the fiber angle color map. **Fig.1B**, **1C**, and **1D** illustrate respectively ellipsoidal, superquadrics, and toroidal representations, with shaded areas highlighting the visual uncertainties specific to each model. **Fig.1E** displays the supertoroidal glyph field, which arises from both variations in genus and shape, illustrating that supertoroids are less prone to visual ambiguity and improve the visualization of the laminar architecture as depicted by the changing distribution of fiber angles. Furthermore, by varying the values of  $\gamma_1$  and  $\gamma_2$ , one may emphasize different structural information, as displayed on an infarcted canine heart in **Fig.2**. **Fig.2B-J** show that depending on the values of  $\gamma_1$  and  $\gamma_2$ , the supertoroidal fields may emphasize, either the *infarcted*, *non-infarcted* and *transition* areas, allowing the discrimination of tissue, as shown within the shaded areas. Hence, a judicious choice of  $\gamma_1$  and  $\gamma_2$  creates a distinct geometrical delineation of the medium and the minor eigenvectors that allows a full understanding of the tensor fields regardless of the visualization perspective.

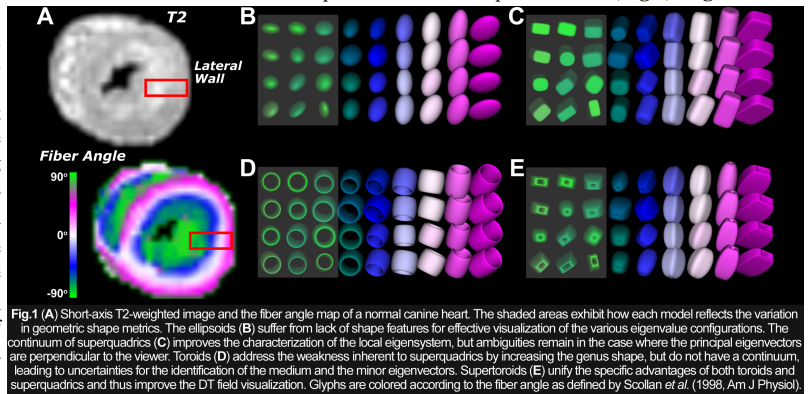


**Fig.1 (A)** Short-axis T2-weighted image and the fiber angle map of a normal canine heart. The shaded areas exhibit how each model reflects the variation in geometric shape metrics. The ellipsoids (B) suffer from lack of shape features for effective visualization of the various eigenvalue configurations. The continuum of superquadrics (C) improves the characterization of the local eigensystem, but ambiguities remain in the cases where the principal eigenvectors are perpendicular to the viewer. Toroids (D) address the weakness inherent to superquadrics by increasing the genus shape, but do not have a continuum, leading to uncertainties for the identification of the medium and the minor eigenvectors. Supertoroids (E) unify the specific advantages of both toroids and superquadrics and thus improve the DT field visualization. Glyphs are colored according to the fiber angle as defined by Scollan *et al.* (1998, Am J Physiol).

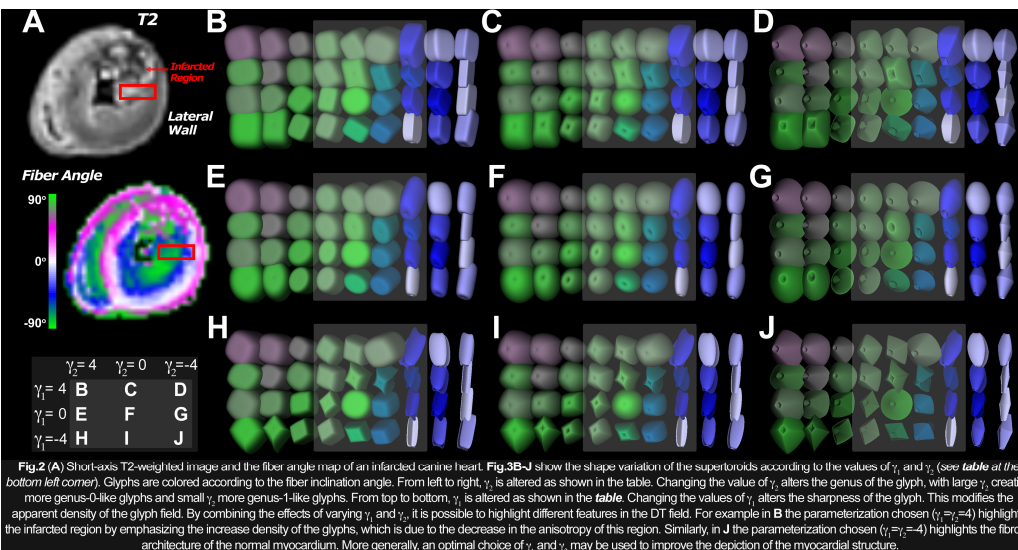


**Fig.2 (A)** Short-axis T2-weighted image and the fiber angle map of an infarcted canine heart. **Fig.2B-J** show the shape variation of the supertoroids according to the values of  $\gamma_1$  and  $\gamma_2$  (see table at the bottom left corner). Glyphs are colored according to the fiber inclination angle. From left to right,  $\gamma_1$  is altered as shown in the table. Changing the value of  $\gamma_2$  alters the genus of the glyph, with large  $\gamma_2$  creating more genus-0-like glyphs and small  $\gamma_2$  more genus-1-like glyphs. From top to bottom,  $\gamma_2$  is altered as shown in the table. Changing the values of  $\gamma_1$  alters the sharpness of the glyph. This modifies the apparent density of the glyph field. By combining the effects of varying  $\gamma_1$  and  $\gamma_2$ , it is possible to highlight different features in the DT field. For example in B the parameterization chosen ( $\gamma_1=4$ ) highlights the infarcted region by emphasizing the increase density of the glyphs, which is due to the decrease in the anisotropy of this region. Similarly, in J the parameterization chosen ( $\gamma_2=-4$ ) highlights the fibrous architecture of the normal myocardium. More generally, an optimal choice of  $\gamma_1$  and  $\gamma_2$  may be used to improve the depiction of the myocardial structure.

## Discussion

The supertoroid-based representation is an evolution of the toroidal model that enhances the three-dimensional perception of biological tissue structure and organization using DT-MRI. By means of different sets of supertoroidal shape parameters, our model facilitates the understanding of the underlying myocardial structural properties. Further studies on normal and pathological specimen may optimize the choice of parameters  $\gamma_1$  and  $\gamma_2$  in order to strengthen the classification of tissue-specific nature. In conclusion, the *supertoroidal* model, as a superset of genus-0 and genus-1 shapes, improves the effectiveness of the diffusion tensor characterization of biological tissues.

**Acknowledgments:** Sponsored by NIH grant HL078650 and the Brown-Coxe Fellowship.

**References:** [1] Mekkaoui C *et al* SCMR 2008 [2] Mekkaoui C *et al* ISMRM 2008 [3] Ennis DB *et al* MRM 2005 [4] Westin C-F *et al* ISMRM 1997